Modelled carbon fluxes as validated by field data on the north Norwegian shelf during the productive period in 1994

Dag Slagstad, Kurt S. Tande & Paul Wassmann

SARSIA

Slagstad D, Tande KS, Wassmann P. 1999. Modelled carbon fluxes as validated by field data on the North Norwegian shelf during the productive period in 1994. *Sarsia* 84:303-317.

A 3-dimensional coupled hydrodynamic and biological model has been used to study the effect of the physics on the productivity and the carbon export of the ecosystem outside Troms county, northern Norway. The horizontal grid point distance is 4 km. The ecosystem model consists of eight state variables (nitrate, ammonium, silicate, diatoms, flagellates, microzooplankton, fast sinking detritus, slow sinking detritus) and assumes that nitrogen and silicate are the limiting nutrients. Measured mesozooplankton biomass (mainly *Calanus finmarchicus*) is used to impose the effect of grazing. The parameters used by the model are mostly taken from the literature, but monthly measurements of CTD, nutrients, chlorophyll, micro- and mesozooplankton, and sedimentation have been used to validate the model output. The measured data were compared and contrasted with two model scenarios (i.e. without and with advection), where the latter run was in best agreement with the field data. This may be due to a more realistic physical setting, since without advection, the nutrient supply comes only via vertical mixing, while with advection nutrients are being advected into the euphotic zone via topographically steered upwelling. These upwelling "hot spots" are found downstream with an elevated annual production > 160 g C m^{-2}, of which 70 % is new production. Comparing the partitioning of carbon between the components in the pelagic food webs in the Bering Sea and the north Norwegian shelf, the highest similarity in species assemblages may exist between the outer Bering Sea shelf and the north Norwegian shelf. The mesozooplankton carbon flow in both areas is calculated to approximately 60 g C m^{-2} yr^{-1}. An important difference in the routing of the flow is present, where at the Norwegian shelf mesozooplankton grazing in the model was fuelled exclusively by microzooplankton. The modelled carbon fluxes outside North Norway during the study period may be influenced by topography, and the highest phytoplankton crop is found near the high productive area, close to the shelf break after the spring bloom. The banks (as Nordvestbanken) receive much of their water from the adjacent shelf region, which in general has less biomass than the shelf break. The trenches like Malangsdjupet receive most of their water from the shelf break and will therefore in general tend to have net import of biomass which sinks out to deeper layers where the residence time is longer.

Dag Slagstad, SINTEF Civil and Environmental Engineering, N-7465 Trondheim, Norway. – Kurt S. Tande & Paul Wassmann, Norwegian College of Fishery Science, University of Tromsø, N-9037 Tromsø, Norway.
E-mail: dag.slagstad@civil.sintef.no – kurtt@nfh.uit.no – paulw@nfh.uit.no

Keywords: North Norwegian shelf; physical-biological modelling; plankton; carbon budget.

INTRODUCTION

The continental shelves are situated between land and open oceans and have become refuse pits of developed nations at the same time as they are nursery grounds for the most important fish stocks in the world. A growing awareness of the importance of these regions for the bordering societies has led to several recent multidisciplinary research programs, with the EU funded program Ocean Margin Exchange Processes (OMEX) focusing on carbon fluxes on the Western European shelves as one example.

Boreal shelf structures are subjected to high variability in the physical forcing where temperature, nutrients, and light climate vary extensively through the year (Hopkins & al. 1984). In addition to this, the shelf ecosystems are a strong advective regime with surface currents close to 50 cm s^{-1} in several regions (Nordby & al. 1999). The carbon dynamics of topographically complex and variable hydrodynamic shelf ecosystems can therefore by no means be understood on the basis of field data alone due to inadequate sampling methods in space and time (see Walsh 1988). Model approaches, resting as much as possible on sound data, are therefore needed to scale for instance carbon fluxes in these areas.

In North Norwegian waters, most of the recent investigations regarding the trophodynamics of the marine pelagic systems have been carried out in the coastal

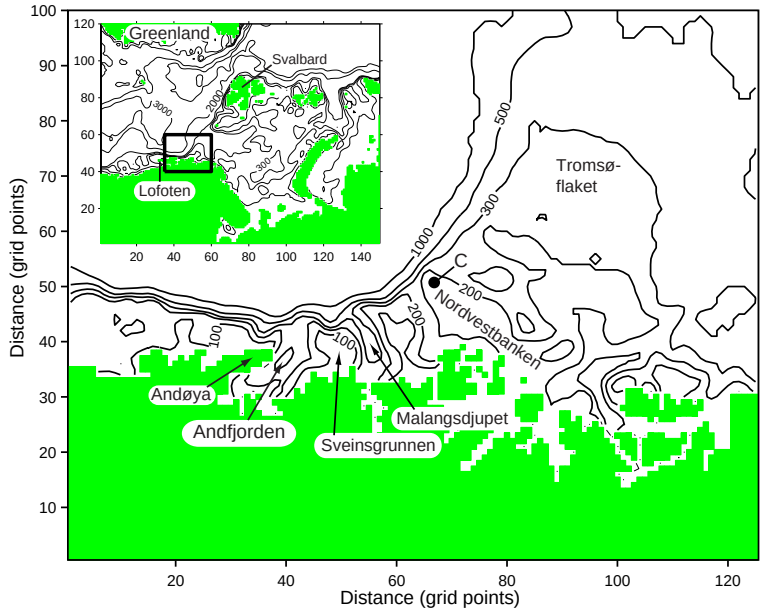

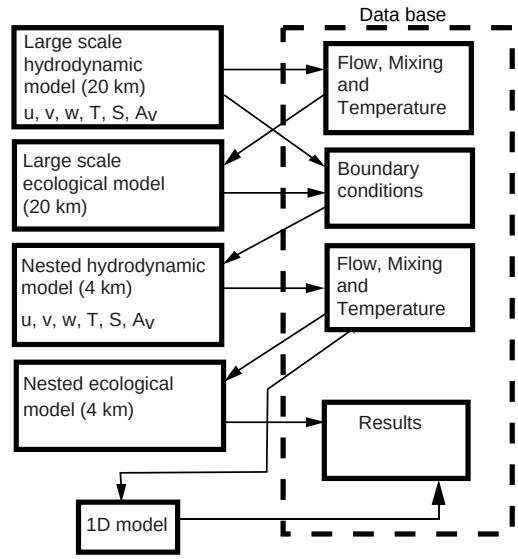

Fig. 1. Model domains (upper panel) . The inserted figure shows the area covered by the large scale model (20 km) and the nested model domain is shown by a rectangular box. Selected isobaths are indicated, as well as Stn C at Nordvestbanken. Simulator structure (lower panel).

zone and fjords of northern Norway (e.g. Eilertsen & Taasen 1984; Hopkins & al. 1989; Tande 1991; Hegseth & al. 1995; Wassmann & al. 1996). Although some offshore investigations were carried out in the Norwegian Sea during the 1950s (e.g. Halldal 1953; Sverdrup 1953; Braarud & al. 1958), little is known about plankton dynamics and sedimentation processes off the north Norwegian shelf, (but see Sætre & Mork 1981; Rey 1981a, 1981b; Peinert 1986; Peinert & al. 1987). To the best of our knowledge, up to now, no simultaneous studies of the cycles of nutrients, phytoplankton, zooplankton, and suspended matter have been undertaken on and off the north Norwegian shelf covering the entire productive season. The field study within the scope of OMEX was therefore highly warranted (e.g. Andreassen & al. 1999; Nordby & al. 1999; Ratkova & al. 1999; Wassmann &

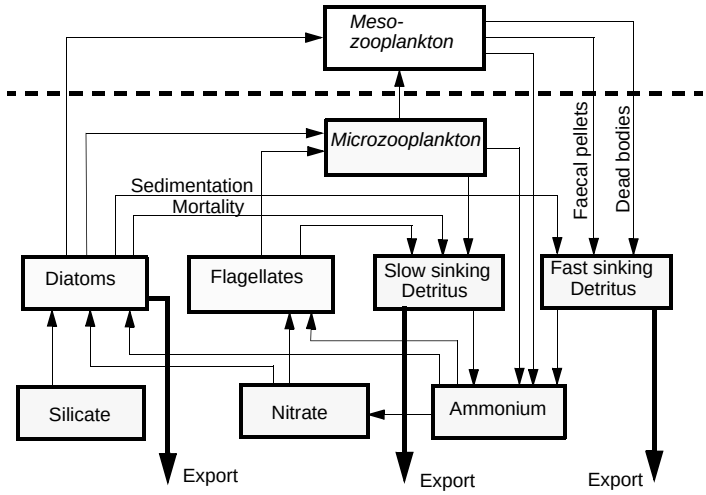

Fig. 2. Conceptual ecosystem model.

al. 1999) and leads up to the present paper which is a validation of a coupled biological-physical model.

Here we address several questions pertinent to the dynamics of lower trophic levels in boreal waters: Is it possible to establish a simplified coupled physical-biological model which mirrors the seasonal variation (i.e. from March to September) in the measurements of the principal components investigated in our field program? After having critically compared the model with our field data, we then applied the model in order to address the following:

1. Is the primary production partitioned reasonably between the components defined in the model, and how does the calculated carbon budget fit to other shelf areas as for instance the Bering Sea?
2. Is there good coherence between the physical conditions and the estimated primary production in the study region outside North Norway?
3. By using two contrasting topographical settings, a bank (Nordvestbanken) and a trench (Malangsdjupet) we investigate how the local variations in topography modify the seasonal variation in the lateral carbon fluxes (i.e. from March to September).

MODEL DESCRIPTION

Hydrodynamic model

The hydrodynamic model is based on the primitive Navier-Stokes equations solved by a finite difference scheme. The model uses the z-coordinates in the vertical direction (i.e. each model level has a fixed thickness except for the surface level and the one close to the bottom). A detailed model description is found in Støle-Hansen & Slagstad 1991 and Moseidjord & al. 1999). The model domain covers an area of 500×400 km^2 off the coast of Northern Norway (Fig. 1). The horizontal grid point distance is 4 km and 20 vertical levels. The thickness of the levels from the surface is: 10 m, 6×5 m, 10 m, 6×25 m, 2×50 m, 100 m, 200 m, 400 m, 2000 m. The open boundary conditions for this (nested) model is generated by a regional model covering most of the Norwegian Sea and the whole Barents Sea (Slagstad & Wassmann 1996). The coupling between the models is performed by a flow relaxation scheme (Martinsen & Engedahl 1987). The horizontal grid point distance is 20 km and the vertical resolution is the same as for the nested model. At the open boundaries, the current velocities are specified (Slagstad & al. 1999), and temperature and salinity are taken from the monthly Levitus (1982) database.

Atmospheric forcing is the same for both models. Wind and air pressure input is taken from the Norwegian Meteorological Institute's hindcast data archive (Eide & al. 1985) for the year 1994. The heat flux is calculated from air temperature, humidity, cloud cover that is interpolated from available meteorological stations within the model domain and the theoretical height of the sun. Initial values of temperature and salinity were taken from the Levitus database (Levitus 1982). Freshwater input is calculated from average seasonal run-off (Tollan 1974). Advection of any scalar property c is performed by the advection-diffusion equation

$$\frac{\partial c}{\partial t} + Adv(c) + Diff(c) = G \qquad (1)$$

where G is the local rate of change of a constituent (e.g. temperature, salinity or a biological state variable). The

two operators, *Adv* and *Diff* represent the advection and the diffusion terms, respectively, which are defined as:

$$Adv(c) = \frac{\partial}{\partial x}(uc) + \frac{\partial}{\partial y}(vc) + \frac{\partial}{\partial z}(w + w_b)c \qquad (2)$$

$$Diff(c) = -K_h \nabla^2 c - \frac{\partial}{\partial z} K_v \frac{\partial c}{\partial z} \qquad (3)$$

where t is time, x, y, z are the three spatial coordinates, u, v, and w are the current speed in x, y, z directions, respectively; K_h and K_v are the horizontal and vertical eddy diffusion coefficients. For later use we define the combined advection-diffusion term $AD = Adv + Diff$. K_h is taken to be constant, 200 $m^2\ s^{-1}$ for the regional model and 10 $m^2\ s^{-1}$ for the nested model. The vertical eddy diffusion is calculated from the Richardson number and a simplified surface wave model (Slagstad & Wassmann 1996).

Ecological model

The model structure chosen here is based on the field investigations performed in the region in 1994 (Andreassen & al. 1999; Halvorsen & Tande 1999; Ratkova & al. 1999; Wassmann & al. 1999a; Wassmann & al. 1999b; Urban-Reich & al. 1999; Verity & al. 1999). The ecosystem model assumes that nitrogen and silicate are the potential limiting nutrients on the North Norwegian shelf and consist of eight state variables (Fig. 2). These compartments are: nitrate (No_3), ammonium (*Na*), silicate (*Si*), diatoms (*Di*), flagellates (*F*), microzooplankton (*Mi*), fast sinking detritus (*Df*), slow sinking detritus (*Ds*). The mesozooplankton (*Me*) is dominated by *Calanus finmarchicus* and we have used the interpolated biomass values based on monthly sampling interval in order to specify the grazing pressure (see below). The basic unit used in the model is mmol N m^{-3}. When conversion to carbon is needed, the Redfield ratio (Redfield & al. 1963) is applied. An initial (winter value) concentration of nitrate was specified to 10 mmol m^{-3}.

The phytoplankton growth is a function of light, nutrients and temperature and will vary with solar elevation (i.e. the season, latitude and the time of the day) and position in the water column. A relationship between the solar elevation and photosynthetic available irradiance (PAR) has been established by using a model of Bird (1984). The attenuation coefficient, k, of light in the water column is described by Parsons & al. (1983):

$$k = \{k_w + 0.0088Chl + 0.054(Chl)^{2/3}\} / \bar{\mu} \qquad (4)$$

where k_w (m^{-1}) represents the attenuation coefficient of pure seawater (Smith & Baker 1981), *Chl* is the concentration of chlorophyll *a* and $\bar{\mu}$ is the average cosine of the light field that equals 0.6 (Kirk 1983). Using this operator as defined by equations 1-3, we can write the model equations as shown in Table 1.

Table 1. Model Equations.

(8) $$\frac{\partial Di}{\partial t} + AD(Di) = Di[P^B_{Di}(T)\ \min\{f_I, G^{Di}_N, G_{Si}) - \mu_{Di} - S(No3, Na, Si)] - G^{Di}_{Me} - G_{Mi}$$

(9) $$\frac{\partial F}{\partial t} + AD(F) = F[P^B_F(T)\ \min\{f_I, G^F_N\} - \mu_F] - G_{Mi}$$

(10) $$\frac{\partial No3}{\partial t} + AD(No3) = -DiP^B_{Di}(T)\ \min\{f_I, G^{Di}_N, G_{Si}\} - FP^B_F(T)\ \min\{f_I, G^F_N\} + \phi_{An} Na$$

(11) $$\frac{\partial Na}{\partial t} + AD(Na) = -DiP^B_{Di}\ \min\{f_I, G_N, G_{Si}\} - FP^B_F\ \min\{f_I, G_N\} - \phi_{Na} Na + MeE_{Me} + MiE_{Mi} + \gamma_{Ds} Ds + \gamma_{Df} Df$$

(12) $$\frac{\partial Mi}{\partial t} + AD(Mi) = Mia_{Mi}\{G^{Di}_{Mi} + G^F_{Mi}\} - E_{Mi}(Di, F) - \gamma_{Mi}] - MeG^{Mi}_{Me}(Di, Mi)$$

(13) $$\frac{\partial Ds}{\partial t} + AD(Ds) = Mi(1 - a_{Mi}) \times (G^{Di}_{Mi} + G^F_{Mi}) + \mu_{Di} Di + \mu_F F - \gamma_{Ds} Ds$$

(14) $$\frac{\partial Df}{\partial t} + AD(Df) = DiS(No3, Na, Si) + (1 - a_C)\, Me - \gamma_F Df$$

Nutrient limitation on growth rate of diatoms and flagellates are calculated by a Michaelis-Menten equation. Nitrogen to support primary production is supplied from two sources, nitrate and ammonium and we assume that the limitation is the total nitrogen available (Fasham & al. 1990). The following expression is used for nitrogen limitation

$$G_N = \frac{No3}{k_N + No3} e^{-\psi Na} + \frac{Na}{k_N + Na} \quad (5)$$

where k_N is the half saturation constant for uptake of nitrate and ammonium, ψ is a parameter determining the suppression of nitrate uptake in presence of ammonium. For diatoms, the nutrient limitation is the minimum of nitrogen, silicate or light limitation.

The loss of diatoms due to sedimentation of resting spores and aggregates is assumed to be caused by nutrient depletion. This, in nature, complex process is described by a formula given in Wassmann & Slagstad

Table 2. Parameters used in the biological model.

Variable	Value	Units	Meaning
α^B_{Di}	0.02	mg C (mg Chl*a*)$^{-1}$ h^{-1} (mmol m^{-2} s^{-1})$^{-1}$	Chlorophyll *a*-normalised photosynthetic efficiency of diatoms
α^B_{F}	0.035	mg C (mg Chl*a*)$^{-1}$ h^{-1} (mmol m^{-2} s^{-1})$^{-1}$	Chlorophyll *a*-normalised photosynthetic efficiency of flagellates
P^B_{mDi}	1.05	mg C (mg Chl*a*)$^{-1}$ h^{-1}	Chlorophyll *a*-normalised maximum gross photosynthetic rate of diatoms
P^B_{mF}	2.0	mg C (mg Chl*a*)$^{-1}$ h^{-1}	Chlorophyll *a*-normalised maximum gross photosynthetic rate of flagellates
N_C	0.16	-	Nitrogen to carbon ratio
Chl*a*_C$_{Di}$	0.03	-	Chl *a* : C ratio in the diatoms
Chl*a*_C$_{F}$	0.02	-	Chl *a* : C ratio in the flagellates
k_N	0.4	mmol m^{-3}	Half-saturation constant for nitrate
μ_{Di}	0.05	d^{-1}	Mortality rate of diatoms
μ_F	0.05	d^{-1}	Mortality rate of flagellates
g^{Mi}_{max}	0.63	d^{-1}	Maximum specific grazing rate of microzooplankton on flagellates at 0 °C
$C^{F\,/\,Di}_{ThrMi}$	5/5	mg C m^{-3}	Lower feeding threshold for microzooplankton feeding on flagellates and diatoms, respectively
$C^{F\,/\,Di}_{CriMi}$	30/30	mg C m^{-3}	Critical concentration for microzooplankton feeding on flagellates and diatoms, respectively
$C^{Mi\,/\,Di}_{ThrMe}$	5/10	mg C m^{-3}	Lower feeding threshold for mesozooplankton feeding on microzooplankton and diatoms, respectively
$C^{Mi\,/\,Di}_{CriMe}$	20/100	mg C m^{-3}	Critical concentration for mesozooplankton feeding on microzooplankton and diatoms, respectively
μ_3	0.05	d^{-1}	Mortality rate of microzooplankton
a_{Mi}	0.7	-	Assimilation efficiency of microzooplankton
k_w	0.04	m^{-1}	Attenuation coefficient for pure sea water
a_{Me}	0.7	-	Assimilation efficiency of mesozooplankton
ψ	1.4	(mmol N m^{-1})$^{-1}$	Parameter describing the inhibition effect on nitrate uptake by ammonium
dmn	0.004	h^{-1}	Parameter (Eqn 6)
dmx	0.02	h^{-1}	Parameter (Eqn 6)
dg	0.1	-	Parameter (Eqn 6)

(1993) which transform diatoms into the compartment of fast sinking detritus

$$S = (d_{mn} + (d_{mx} - d_{mn}))e^{-\min\{G_N^{Di}, G_{Si}^{Di}\}/d_g} \quad (6)$$

where S is the specific rate of conversion from diatoms to fast sinking detritus, d_{mn}, d_{mx} and d_g are parameters given in Table 2. A constant specific rate of dead diatoms and flagellates (often associated with respiration) are turned into slow sinking detritus.

The functional relationship of the photosynthetic active radiation (I_z) and the specific photosynthetic rate (f_I) is described by the following formula

$$f_I = 1 - e^{-\alpha^B I_z / P_m^B} \quad (7)$$

where α^B is the chlorophyll *a*-normalised photosynthetic efficiency and P_m^B is the chlorophyll *a*-normalised maximum gross photosynthetic rate (see also Jassby & Platt 1976; Sakshaug & Slagstad 1991).

An apparently important grazer in the investigated area is microzooplankton. This functional group consists of several species, which vary in biomass during the season (Ratkova & al. 1999; Verity & al. 1999). Microzooplankton is usually assumed to feed on flagellates (Hansen & al. 1993), but observations on diatom grazing have also been observed (Nejstgaard 1994). Here we assume that microzooplankton prefer flagellates. Mesozooplankton consumes microzooplankton in this context represented by *C. finmarchicus*, which was found to dominate the mesozooplankton biomass during the period of study (Halvorsen & Tande 1999). We have not modelled this species dynamically, but used linearly interpolated measured biomass values (see below) as a forcing function in the model. *C. finmarchicus* is assumed to feed both on diatoms and microzooplankton. The biomass of the mesozooplankton is specified, but its impact on the ecosystem through grazing, excretion and fecal pellets production is simulated. Since the mesozooplankton is dominated by *Calanus*, parameters for this functional group will be closely related to this species in the model. The species has a high biomass in spring and early summer. In June *C. finmarchicus* already starts to migrate to deep water and its biomass decreases, in accordance with the mesozooplankton biomass which has been found to stay close to the surface during the spring but shift gradually towards the depth during the summer (see Falkenhaug & al. 1997; Halvorsen 1997). This is modelled as a reduction in the active biomass involved in the ecological interactions in the euphotic zone. Monthly, spatial averaged biomass values (Table 3) were interpolated in time. It was further assumed that half of the biomass found below 50 meters was actively feeding in the surface layer.

The mesozooplankton was allowed to graze on both diatoms G_{Me}^{Di} and microzooplankton G_{Me}^{Mi}, following a functional relationship described by Carlotti & Radach (1996). Maximum grazing rate was set equal to 24% of body weight per day. A linear functional relationship between available food and grazing were used. On the other hand, if the maximum grazing rate at a given temperature cannot be sustained, the additional food is taken from diatoms. A linear functional relationship is used (see Table 2), starting from a lower feeding threshold (C_{Thr}^{Mi}) and levels out at the critical concentration (C_{Cri}^{Mi}). Grazing on diatoms started at a lower threshold value of 10 mg C m^{-3} and a critical concentration of 100 mg C m^{-3} was set, whereas the corresponding grazing parameters for microzooplankton were 7 mg C m^{-2} and 20 mg C m^{-3}. The assimilation efficiency (a_{Me}) was equal to 0.7 and the excretion rate (E_{Me}) was 10 % of the grazing rate + 1 % of the mesozooplankton biomass per day.

Detritus is divided into a slow and a fast sinking component. The slow sinking component encompass non-assimilated material, dead bodies from microzooplankton and dead diatoms and flagellate cells, whereas the fast sinking component is made up by fecal pellets and dead bodies from mesozooplankton and sedimenting diatom cells (resting spores, aggregates, etc.). The fast sinking component has a sinking rate of 50 m d^{-1} and degradation rate of 0.33 d^{-1}, whereas the slow sinking component has a sinking rate of 1 m d^{-1} and a degradation rate of 0.05 d^{-1} (see Table 1 for model equations).

SIMULATED RESULTS

The model is run according to the above specification along the following simulation steps (see also Fig. 1, lower panel):

1. Regional model for a period of about eight months and with saving the boundary conditions for the nested hydrodynamic model.
2. Nested hydrodynamic model with saving daily average of flow field, temperature and vertical mixing coefficients.

Table 3. Monthly average biomass (g C m^{-2}) of copepods from the shelf within the study region outside Troms.

Depth intervall	March	April	May	June	July	August	September
0-50 m	0.16	0.29	7.13	1.26	0.96	0.8	1.6
50 m – bottom	0.16	0.95	0.64	2.43	1.87	2.0	0.81

3. Regional ecological model using no gradient as the open boundary conditions for the biological state variables. The boundary conditions for the nested model domain are being saved.
4. Nested ecological model takes input from the previous simulated flow fields, boundary conditions and cloud cover and produce results which are saved for later analysis. Typical time for one simulation run (7 months) is 4 days on an Ultra Sparc workstation.

Station C without advection

In order to test the dynamic behaviour of the ecological model a 1D scenario was run. Simulated time series of temperature and vertical eddy diffusion coefficients from a position corresponding to Stn C on Nordvestbanken (Fig. 1) were used as input. The primary production started in March and increased rapidly to 1 g C m^{-2} d^{-1} in mid April, when deepening of the mixed layer reduced the production again. The spring bloom reached a maximum production of (3.6 g C m^{-2} d^{-1}) around 20 May (Fig. 3 F) and terminated due to nitrate limitations a few days later. During the following summer the nitrate concentration in the upper 30 m was below 1 mmol m^{-3}, but the surface concentration of silicate remained high (above 4.5 mmol m^{-3}). The production showed large fluctuations as a result of mixing events, bringing nutrients into the euphotic zone with average values around 0.5 g C m^{-2} d^{-1}. The phytoplankton was dominated by flagellates. In late May, when the microzooplankton was controlled by mesozooplankton grazing, concentrations of flagellates up to 6 mmol N m^{-3} (i.e. 450 mg C m^{-3}) were found (Fig. 3C). When the grazing pressure from mesozooplankton was reduced in June and the biomass of microzooplankton increased, the flagellate concentration was reduced to about 15 mg C m^{-3}.

Total, annual primary production was estimated to 137 g C m^{-2}, of which 58 % was new production. It is important to note that only 17 % of the production were provided by diatoms. Total export through a 75 m surface was 32.3 g C m^{-2} yr^{-1} while 27.5 g C m^{-2} yr^{-1} reached the bottom at 147 m. Integrated mesozooplankton grazing was 48 g C m^{-2} yr^{-1}.

Station C with advection

The outcome of the 3D simulation (Fig. 4) demonstrates that the surface nitrate was depleted in a short period at the end of May. Average surface nitrate was 2 mmol m^{-3} during the period, although values less than 1 mmol m^{-3} were also found. The utilisation of silicate is about the same as in the non-advection scenario, with a diatom fraction of total production estimated to 22 %.

The variation in concentration of diatoms was low and values in the mixed layer were between 10 and 20 mg C m^{-3} from early April to September. The flagellates were found in high concentrations (up to 400 mg C m^{-3}) from late May to mid June in a period where the mesozooplankton concentration was high. After this period mixed layer concentration was around 15 mg C m^{-3}.

An elevated primary production was observed in this run totalling to 164 g C m^{-2} yr^{-1} of which 66 % was new production. Total export through a 75 m surface was 40.1 g C m^{-2} yr^{-1} and 30.5 g C m^{-2} yr^{-1} reached the bottom at 147 m. The mesozooplankton grazed 43 g C m^{-2} yr^{-1} that mostly was obtained on microzooplankton. Microzooplankton grazing on flagellates and diatoms was integrated to 61.4 and 10.6 g C m^{-2} yr^{-1}, respectively.

DISCUSSION

In the present model we have obtained modelled data which can be compared and contrasted with field observations from 8 cruises of one week duration each separated by approximately one month (see Nordby & al. 1999) during the simulation period. The validation of the model should be conducted by great care, since great variability in the spatial distribution of phytoplankton has been found on the Northern Norwegian shelf even when sampled within time intervals of days with spatial resolution less then two nautical miles (see for instance Babichenko & al. 1999). In the following we discuss the validation of model results in two separate scenarios, with and without advection.

Validation at Station C without advection

The modelling results derived from Stn C without advection (Fig. 3) indicate clearly that large differences exist between modelled and observed data during 1994. For example, the model nitrate is depleted in the surface layers in May while that rarely was the case in the field (see Wassmann & al. 1999), but the modelled distribution of silicate is more coherent with the data. The phytoplankton carbon was dominated by flagellates (81-99 % of biovolume), while that of diatoms was low (Ratkova & al. 1999) as predicted. The modelled bloom of flagellates in May and June with a predicted maximum of 450 mg C m^{-3} spreading from the surface down to 60 m depth is opposed by field data, which revealed maximum average concentration in the upper 100 m of 50 mg C m^{-3} (Ratkova & al. 1999). The field data demonstrated that no major accumulation of phytoplankton (in terms of diatom chlorophyll and flagellates) occurred on the shelf during the productive period in 1994 (see Wassmann & al. 1999; Ratkova & al. 999). Also the distribution pattern and the concentration of microzooplankton predicted by the model differ from the data, but the predicted vertical flux of carbon was similar to

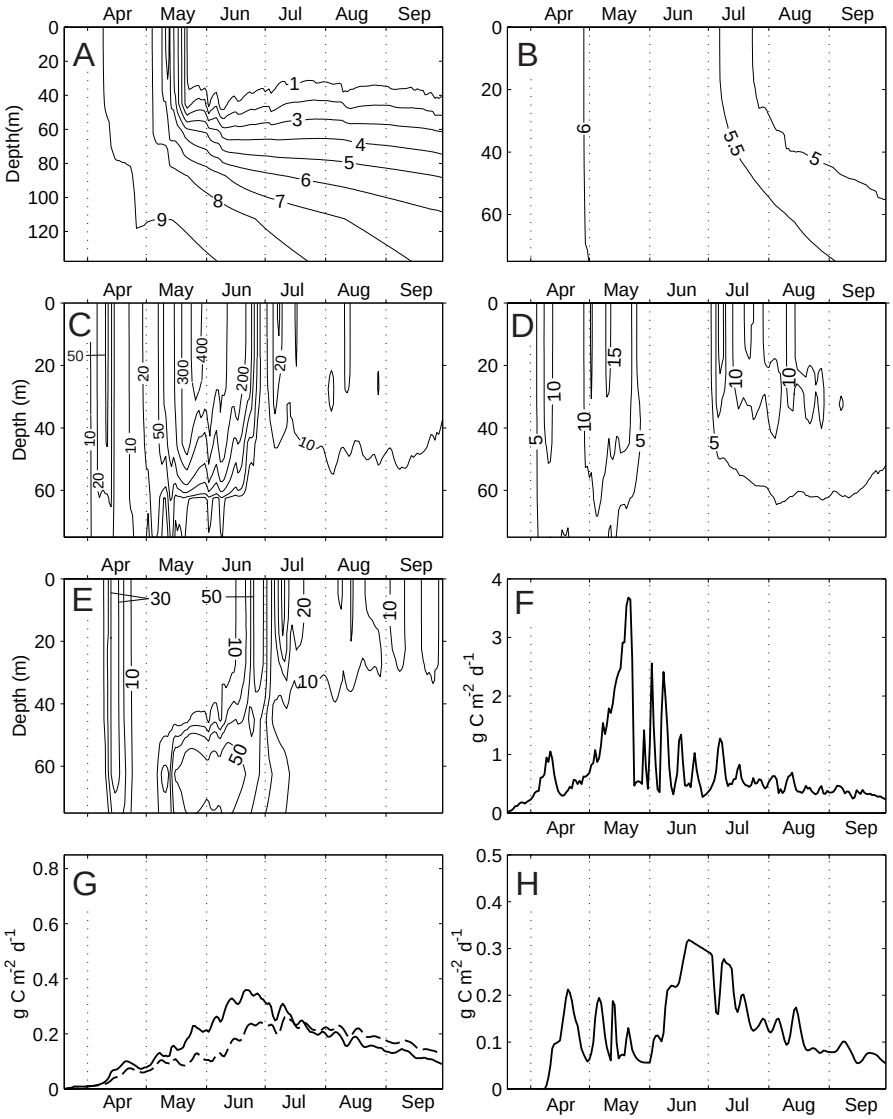

Fig. 3. Model dynamics at Stn C on Nordvestbanken without advection. A. Nitrate (mmol N m^{-3}). B. Silicate (mmol m^{-3}). C. Flagellates (mg C m^{-3}). D. Diatoms (mg C m^{-3}). E. Microzooplankton (mg C m^{-3}). F. Total primary production (g C m^{-2} d^{-1}). G. Solid line, export through the 75 m surface and as dashed line, export to the bottom (g C m^{-2} d^{-1}). H. Net "export" to mesozooplankton (g C m^{-2} d^{-1}).

the patterns observed on the shelf (Andreassen & al. 999). Obviously the prediction by the model at Stn C under the exclusion of advection is not well validated by observed data.

Validation of Station C with advection

The model at Stn C with advection reflects the observed data far better. The decline of silicate is slow and both nitrate and silicate are not depleted in the surface layers (Fig. 4). The biomass of the flagellates dominates the phytoplankton biomass, while diatoms never accumulate in great numbers, except during summer in the surface layers. Microzooplankton accumulates in June/July and the rates and patterns of vertical carbon export at 75 m fit well to those recorded during the field investigation (Andreassen & al. 1999). Both the time and depth variations of vertical carbon export, as well as the rates are well mirrored by the model. The seasonal

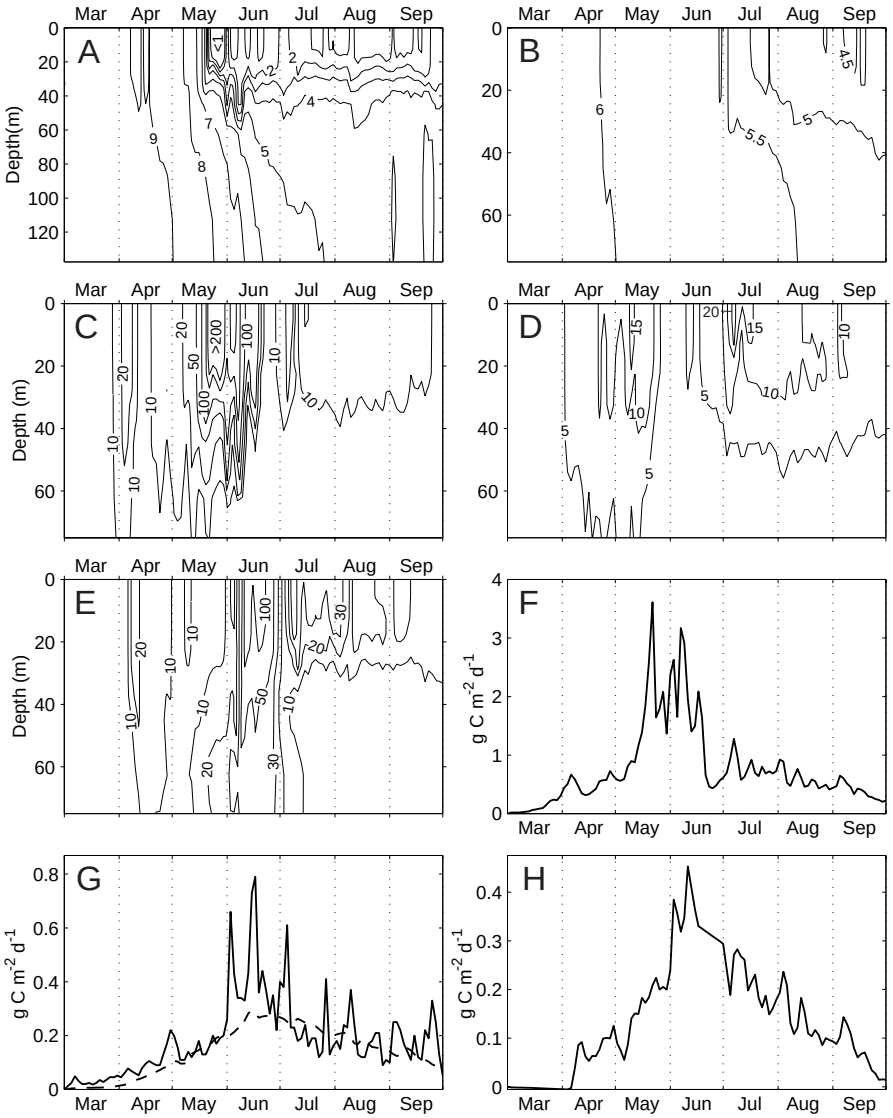

Fig. 4. Model dynamics at Stn C with the full 3D model run. A. Nitrate (mmol N m^{-3}). B. Silicate (mmol m^{-3}). C. Flagellates (mg C m^{-3}). D. Diatoms (mg C m^{-3}). E. Microzooplankton (mg C m^{-3}). F. Total primary production (g C m^{-2} d^{-1}). G. Solid line: export through the 75 m surface, dashed line: export to the bottom (g C m^{-2} d^{-1}). H. Net "export" to mesozooplankton (g C m^{-2} d^{-1}).

mesozooplankton grazing rate fits well to rough calculations presented by Verity & al. (1999). The reasons for the improved coherence between modelled and observed data when advection is being introduced may have several reasons. One feature which we would like to emphasis is that in the non-advection case, nutrient supply comes only via vertical mixing, while with advection nutrients are being advected into the euphotic zone via topographically steered upwelling (Moseidjord & al. 1999). This latter mechanism for upwelling occurs in areas which is situated mainly at the entrance to Malangsdjupet, 2-3 days upstream to our Stn C (see Fig. 1) and provide a time period which is well within the response time for phytoplankton.

While many of the dominant patterns, concentrations and rates seem adequately reflected in the model with advection, not all the predictions are in accordance with the observations. The minimum silicate contact concen-

tration was lower and the concentrations of flagellates, diatoms and microzooplankton (Ratkova & al. 1999; Wassmann & al. 1999) higher compared to the model. Why is this so? One reason could be that the model is set to represent Stn C while the field observations used in the validation are close to the shelf edge. High fluctuation is observed between various sites across the shelf, where for instance copepod biomass was found to differ by a factor of 2-3 in, and around, Malangsdjupet during a sampling interval of 2-4 days (Babichenko & al. 1999; K.S. Tande, unpublished). The inherent variability driven by the instability of the model, the analytical precision of the various variables and the restrictions in the sampling design and frequency will obviously affect the observed differences between the model and the field data. Nevertheless, the model seems to reflect the ecosystem dynamics at the shelf of Nordvestbanken to an acceptable and adequate extent. In the following we have used the modelled data to address the three objectives stated in the *Introduction*.

ANALYSIS OF MODELLED DATA

Carbon budget

In order to compare the modelled carbon flow with published data from other boreal regions, we have compared data from our model with calculated rates from the Bering Sea shelf (Table 4). The different annual carbon budgets from the outer and middle Bering Sea shelf are clearly rooted in different trophodynamic structures in the pelagic community (Walsh & McRoy 1986). The outer shelf is close to an oceanic basin, which acts as an overwintering site for large copepods. The simulated annual primary production is about the same for the North Norwegian shelf as found for the outer and middle Bering Sea shelf. The winter nutrients concentrations on the North Norwegian shelf is less than half those of Bering Sea shelf (Whitledge & al. 1986; Wassmann & al. 1999a). Therefore, a large fraction of the annual primary production on the North Norwegian shelf is based on nutrient supplied to the euphotic zone after the spring bloom. On the outer shelf primary production supports an essentially pelagic food web, with a strong component of zooplankton grazers or predators like on Nordvestbanken. The situation is reversed on the middle and inner shelves, where less of primary production is grazed by zooplankton but settles instead to the bottom as detritus (Table 4). These differences are rooted in a different composition of grazers, composing two size classes with different life histories. The larger long-lived species, such as *Neocalanus cristatus*, *N. plumchrus*, and euphausiids occupy mostly the outer shelf, while short-lived small organisms such as *Pseudocalanus* spp., *Oithona* spp., and *Acartia longiremis* predominate on the inner and middle Bering Sea shelf (Heinrich 1962; Walsh 1988). At the relatively narrow shelf outside Troms, the site specific differences in species composition are much less prominent than the seasonal shifts. After the seasonal descent of *C. finmarchicus* to deeper waters (300-500 m) in late summer, other species like *Pseudocalanus* spp., *Temora* sp., *Acartia* sp., and *Oithona* sp. will be responsible for the carbon turnover in surface waters (Halvorsen 1997). This shift is not being mirrored in our grazing model. We scaled grazing according to the biomass of *C. finmarchicus*, which is found to compose approximately 80 % of the > 180 µm depth integrated biomass during the study period (Halvorsen 1997; Halvorsen & Tande 1999). This may not fully cover the functional relationship between grazing and ambient food concentrations that are in operation, since the seasonal shifts towards small sized grazers, will promote grazing on small particles (i.e. diatoms) at low concentrations as well.

The highest similarity in species assemblages may exist between the outer Bering Sea shelf and the north Norwegian shelf in 1994, in which the routing of carbon to mesozooplankton has been estimated to approximately 60 g C m^{-2} yr^{-1} in both areas. An important difference in the routing of the flow is present, where on the Norwegian shelf mesozooplankton grazing in the model was being fuelled mainly by microzooplankton (see Table 4). In the model setup we specified mesozooplankton grazing being balanced by a microzooplankton and a diatom source, with two important conditions. Firstly, we defined ciliates being strongly linked to both flagellates and diatoms via a threshold value of 5 µg C l^{-1}, and secondly we modelled the functional relationship between mesozooplankton and diatoms with a lower threshold value of 10 µg C l^{-1} (see Table 2). The functional relationship for the ciliate grazing is in accordance with data obtained from the Sargasso Sea

Table 4. Carbon fluxes on the Bering Sea Shelf (values in g C m^{-2} yr^{-1}) and for the period from March to September for the North Norwegian Shelf (values in g C m^{-2} for the simulation period from 1 March to 30 September) as calculated by the model outlined in the present paper. Bering Sea data adopted from Walsh (1988).
Notes. [1] grazing from mesozooplankton is exclusively mediated via microzooplankton, see text for further explanation.

Group	Bering Sea Shelf		North
	Outer	Middle	Norwegian Shelf
Total primary production	166	166	157
Microzooplankton	-	-	100
Mesozooplankton	68	26	- 60 [1]
Detritus (export)	94	130	57

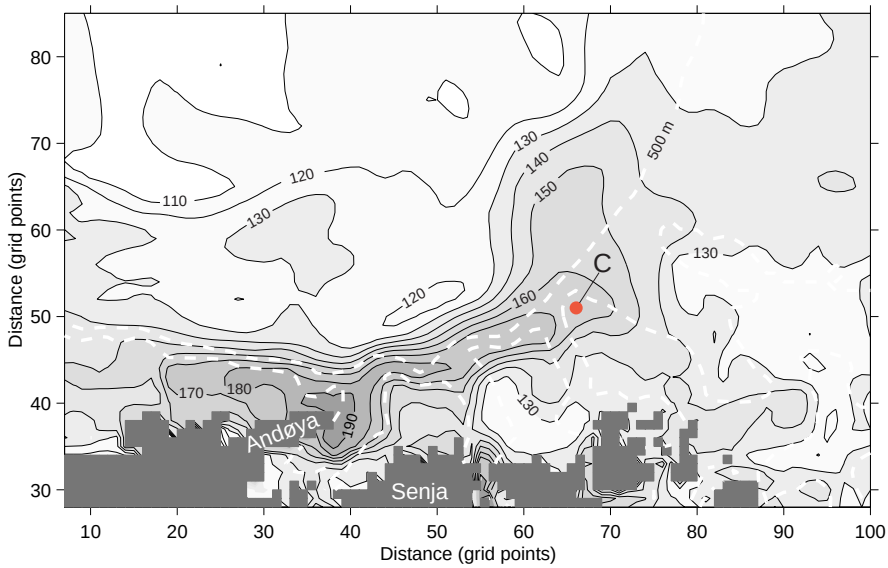

Fig. 5. Annual simulated primary production (g C m^{-2}). The white, broken lines show the 200 m and the 500 m isobaths.

(Lessard & Murrell 1998). The latter threshold is lower than the experimentally determined threshold for copepods from literature (Gamble 1978). Preliminary test runs demonstrated the need to adopt a low threshold value in order to mimic the temporal patterns of a low standing crop of diatoms observed in our field data. A slightly higher lower threshold (about 40 µg C l^{-1}) may have proved to be more adequate, but it may have failed to dramatically increase the flow of carbon between diatoms and mesozooplankton.

During the simulation period the diatom concentration was only occasionally above the lower threshold value defined, which then directed the carbon consumption from mesozooplankton directly to microzooplankton. It is now being established that mesozooplankton graze or, under certain conditions, prefer ciliates as prey (i.e. Stoecker & Capusso 1990; Kleppel 1993; Nejstgaard & al. 1994). Ohman & Runge (1994) showed that a ciliate dominated carbon intake of 2.2-10 % compared to a diatom dominated diet was sufficient to sustain comparable egg production and lipid synthesis in *C. finmarchicus*. On the other hand, in a turbulent area like the north Norwegian shelf the mesozooplankton species are apparently not able to decimate the standing stocks of ciliates. Our investigation during 1994 was not designed to resolve the partitioning of phytoplankton carbon between microzooplankton and mesozooplankton (i.e. the planktonic food chain vs. the microbial food chain) in a scientifically solid way, but the consistent low phytoplankton crop at the shelf from March to September is tantalising.

Spatial differences in production

This scenario demonstrates that there is substantial variability in primary production within the modelled area (Fig. 5) with a maximum annual primary production (ca. 190 g C m^{-2}) found along a band just inside the shelf break (defined by the 500 m isobath). The reason for this could be linked to supply of nutrient rich water via vertical mixing and topographical steered upwelling. Outside Vesterålen, the shelf narrows and the average depth decreases, which will tend to enhance the speed of the coastal current to more than 0.6 m s^{-1} on the average, with maximum modelled velocities well above 1 m s^{-1}. Simulated values correspond reasonably well with ADCP measurements (Orvik & al. 1995; see also Nordby & al. 1999). During the summer, the stratified water masses flowing into this region from south tend to destabilise due to turbulence created by the bottom friction and alternating up and down welling caused by the strong currents flowing on the irregular bottom topography. At the northern tip of Andøya, the Andfjorden trench makes a 400 m deep cross-shelf cut through the shelf. A large fraction of the flow on the shelf (about 45 %) makes a right turn into Andfjorden and flows out again on the southern flank of Sveinsgrunnen. When this westward flowing current meets the strong current at the shelf break, it is forced to flow above the southwestern corner of Sveinsgrunnen (see for instance Nordby & al. 1999, for details of the study site). This topographically steered upwelling acts as a chimney where water, rich in nutrients is supplied to the euphotic zone. The same mechanisms are found at the outlet of

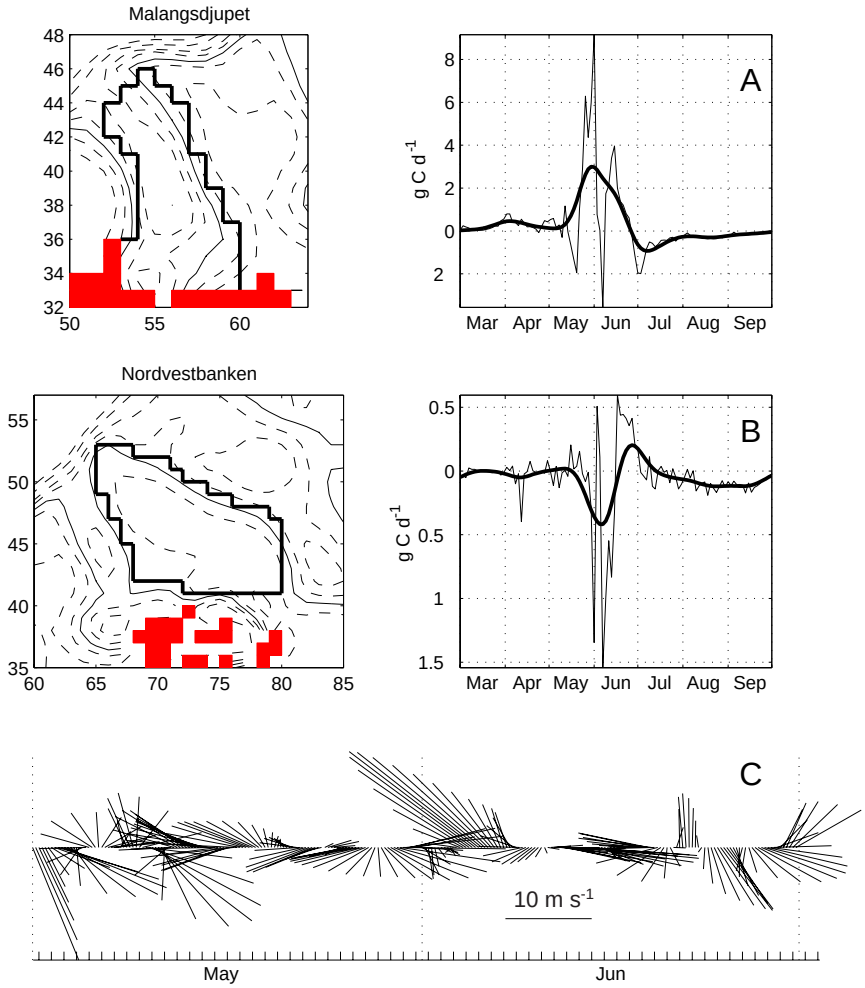

Fig. 6. Time dependent, net organic carbon import to Malangsdjupet (A) and Nordvestbanken (B). The smoothed, thick line was obtained by 10-day low-pass filtering of the total import. The lower panel (C) shows the wind velocity and direction in May-June in the nested model area. The directions of the arrows correspond to the model orientation.

the trenches further north (see Fig. 5), and thus a general feature along the shelf. The upwelling creates also the base for the high new production rate in the areas where most of the primary production is based on nitrate.

Lateral carbon flux

The elevated production found just inside the shelf break (shelf break is defined along the 500 m isobath) is advected into the cross-shelf trenches along their southern slopes. The residence time for water along the high production zone just inside the shelf break is short and a large fraction of the carbon is exported either into the shelf trenches or off-shelf across the shelf break. In Malangsdjupet the simulated, average residence time of surface water is 2.5 days, but increases to more than 10 days below 150 m. Carbon that sinks out from the euphotic zone is likely to be consumed in the region before it is exported. The average net import to Malangsdjupet (Fig. 6A) is 0.29 g C m^{-2} d^{-1} or 62.6 g C m^{-2} yr^{-1} from the outer shelf. This is about 50 % of the new production in the area of Malangsdjupet. Further north, Nordvestbanken area appears to provide a net export of organic carbon (Fig. 6B). The average residence time here is about the same as in Malangsdjupet, but the increase with depth is much smaller. The average net export from the bank is 12.7 g C m^{-2} or 13 % of the new production. The type of this export varies con-

siderably during the study period, with a predominance of phytoplankton in early June and detritus in July-September.

The average, simulated transport of the Norwegian Coastal Current and the Norwegian Atlantic current on the shelf is about 1.3 Sv measured across a section between the northern tip of Andøya and the shelf break. The model simulates a net, average water transport from the shelf break in the investigation area (along a transect of 135 km between Andøya and Nordvestbanken) of 0.22 Sv. The average net export is 12.5 kg C m^{-1} d^{-1} with a maximum of 40 kg C m^{-1} d^{-1} in June. Since the highest production is found just inside the shelf break, a net export of organic carbon off the shelf is expected. The average calculated export during the simulation period is 12.5 kg m^{-1} d^{-1}. There are, however, large differences along the shelf and export values of 350 kg m^{-1} d^{-1} are found outside the northern slope of Malangsdjupet. The highest import values (i.e. onto the shelf) are around 200 kg m^{-1} d^{-1} found at the entrance to Andfjorden and around the northwestern corner of Nordvestbanken.

Most of the net transport of organic matter between the shelf and the oceanic region takes place from mid May to the end of July, during a period where we find the highest biomass and also the greatest horizontal gradients. The noisy pattern that is seen in the lateral transport in June is due to a period with strong shift in wind direction and magnitude which coincide with the time of the year when we have the strongest horizontal biomass gradients. The high activity in the lateral transport of organic carbon was especially pronounced in early June. This was caused by an episode of northeasterly wind pushing the surface shelf water off-shelf. This coincided with a period of high surface biomass of flagellates or microzooplankton producing the signature we observed earlier (see Fig. 4).

Despite the climatological driven variability in the carbon fluxes during the study period, the highest modelled phytoplankton biomass is found near the high productive area close to the shelf break after the spring bloom. The banks (as Nordvestbanken) receive much of their water from the adjacent shelf region, which in general has less biomass than the shelf break. Nevertheless, during short time windows (as seen in June 1994) there may be high net export from the banks due to temporarily elevated biomass at the shelf. The trenches like Malangsdjupet receive most of their water from the shelf break and will therefore in general tend to have net import of biomass which sinks out to deeper layers where the residence time is longer.

ACKNOWLEDGEMENTS

This study was financially supported by the Research Council of Norway (project no. 101323/410 and 108085/122) and the European Commission (MAS2-CT93-0069 OMEX I and MAS3-CT96-0056 OMEX II). We also thank two anonymous referees for valuable comments on the manuscript.

REFERENCES

Andreassen IJ, Wassmann P, Ratkova TN. 1999. Seasonal variation of vertical flux of phytoplankton and biogenic matter at Nordvestbanken, north Norwegian shelf in 1994. *Sarsia* 84:227-238.

Babichenko S, Wassmann P, Poryvkina L, Andreassen IJ. 1999. Small time and spatial scale variability of phytoplankton biomass on the north Norwegian shelf in 1995. *Sarsia* 84:293-302.

Bird RE. 1984. A simple, solar spectral model for direct-normal and diffuse horizontal irradiance. *Solar Energy* 32:461-471.

Braarud T, Gaarder KR, Nordly O. 1958. Seasonal changes in the phytoplankton at various points off the Norwegian west coast. *Fiskeridirektoratets Skrifter Serie Havundersøkelser* 12:1-77.

Carlotti F, Radach G. 1996. Seasonal dynamics of phytoplankton and *Calanus finmarchicus* in the North Sea as revealed by a coupled 1-D model. *Limnology and Oceanography* 41:522-539.

Eide LI, Reiestad M, Guddal J. 1985. *Database av beregnede vind og bølgeparametre for Nordsjøen, Norskehavet og Barentshavet, hver 6. time for årene 1955-81*. Oslo/Bergen, Norway: The Norwegian Meteorological Institute. 38 p.

Eilertsen HC, Taasen JP. 1984. Investigations on the plankton community of Balsfjorden, northern Norway. The phytoplankton 1976-1978. Environmental factors, dynamics of growth and primary production. *Sarsia* 69:1-15.

Falkenhaug T, Tande K, Timonin A. 1997. Spatio-temporal patterns in the copepod community in Malangen, Northern Norway. *Journal of Plankton Research* 19:449-468.

Fasham MJR, Ducklow HW, McKelvie SM. 1990. A nitrogen-based model of plankton dynamics in the oceanic mixed layer. *Journal of Marine Research* 48:591-639.

Gamble JC. 1978. Copepod grazing during the declining spring phytoplankton bloom in the northern North Sea. *Marine Biology* 49:303-315.

Halldal P. 1953. Phytoplankton investigations from weather ship M in the Norwegian Sea, 1948-49. *Hvalrådets Skrifter* 38:1-91.

Halvorsen E. 1997. *Physical and biological factors influencing the seasonal variation in distribution of zooplankton across the shelf at Nordvestbanken, Northern Norway* [Cand.scient. thesis] Tromsø, Norway: University of Tromsø.

Halvorsen E, Tande KS. 1999. Physical and biological factors influencing the seasonal variation in distribution of zooplankton across the shelf at Nordvestbanken, northern Norway, 1994. *Sarsia* 84:279-292.

Hansen FC, Reckermann M, Klein Breteler WCM, Riegman R.1993. *Phaeocystis* blooming enhanced by copepod predation on protozoa: evidence from incubation experiments. *Marine Ecology Progress Series* 102:51-57.

Hegseth E, Svendsen H, Quillfeldt CH von. 1995. Phytoplankton in fjords and coastal waters of northern Norway: environmental conditions and dynamics of the spring bloom. In: Skjoldal HR, Hopkins C, Erikstad KE, Leinaas HP, editors. *Ecology of fjords and coastal waters*. Amsterdam: Elsevier Science. p 45-72.

Heinrich AK. 1962. The life histories of plankton animals and seasonal cycles of plankton communities in the ocean. *Journal du Conseil Internationa pour l' Exploration de la Mer* 27:15-24.

Hopkins CCE, Grotnes PE, Eliassen J-E. 1989. Organization of a fjord community at 70° north: The pelagic food web in Balsfjord, northern Norway. *Rapports et procès-verbaux des réunions. Conseil International pour l'Exploration de la Mer* 188:146-153.

Hopkins CCE, Tande KS, Grønvik S, Sargent JR. 1984. Ecological investigations of the zooplankton community of Balsfjorden, northern Norway: an analysis of growth and overwintering tactics in relation to niche and environment in *Metridia longa* (Lubbock), *Calanus finmarchicus* (Gunnerus) *Thysanoessa inermis* (Krøyer) and *T. raschii* (M. Sars). *Journal of Experimental Marine Biology and Ecology* 82:77-99.

Jassby NG, Platt T. 1976. Mathematical formulations of the relationship between photosynthesis and light for phytoplankton. *Limnology and Oceanography* 21:540-547.

Kirk JTO. 1983. *Light and Photosynthesis in Aquatic Ecosystems*. Cambridge: Cambridge University Press. 401 p.

Kleppel GS. 1993. On the diets of calanoid copepods. *Marine Ecology Progress Series* 99:183-195.

Levitus S. 1982. *Climatological atlas of the word ocean*. NOAA Prof. pap. 13. 173p.

Lessard EJ, Murrell MC. 1998 Microzooplankton herbivory and phytoplankton growth in the northwestern Sargasso Sea. *Aquatic microbial ecology* 16: 173-188.

Martinsen E, Engedahl H.1987. Implementation and testing of a lateral boundary scheme as an open boundary condition in a barotropic model. *Coastal Engineering* 11:603-627.

Moseidjord H, Svendsen H, Slagstad D. 1999. Sensitivity studies of circulation and ocean-shelf exchange off northern Norway. *Sarsia* 84:191-198.

Nejstgaard JC, Witte JH, Wal P van der, Jacobsen A. 1994. Copepod grazing during a mesocosm study of an *Emiliania huxleyi* (Prymnesiophyceae) bloom. *Sarsia* 79:369-377.

Nordby E, Tande KS, Svendsen H, Slagstad D. 1999. Oceanography and fluorescence at the shelf break off the north Norwegian coast (69°20'N-70°30'N) during the main productive period in 1994. *Sarsia* 84:175-189.

Ohman MD, Runge JA. 1994. Sustained fecundity when phytoplankton resources are in short supply: Omnivory by *Calanus finmarchicus* in the Gulf of St. Lawrence. *Limnology and Oceanography* 39:21-36.

Orvik KA., Lundberg L, Mork M. 1995. Topographic influence on the flow field off Lofoten-Vesterålen. In: Skjoldal HR, Hopkins C, Erikstad KE, Leinaas HP, editors. *Ecology of fjords and coastal waters*. Amsterdam: Elsevier Science. p 165-175.

Parsons TR, Takahashi M, Hargrave B. 1983. *Biological Oceanographic Processes*. Oxford: Pergamon Press. 330p.

Peinert R. 1986. Production, grazing and sedimentation in the Norwegian Coastal Current. In: Skreslet S, editor. *The role of freshwater outflow in coastal marine ecosystems*. NATO ASI Series, Vol G7. Berlin: Springer Verlag. p 361-374.

Peinert R, Bathmann U, Bodungen B von, Noji T. 1987. The impact of grazing on spring phytoplankton growth and sedimentation in the Norwegian Current. In: Degens ET, Izdar EI, Honjo S, editors. *Particle flux in the ocean*. Mitteilungen des Geologisch-Paläontologischen Instituts der Universität Hamburg, Sonderband 62, SCOPE/UNEP. p 149-164.

Ratkova TN, Wassmann P, Verity PG, Andreassen IJ. 1999. Abundance and biomass of pico-, nano-, and microplankton on a transect across Nordvestbanken, north Norwegian shelf, in 1994. *Sarsia* 84:213-225.

Redfield AC, Ketchum BH, Richards FA. 1963. The influence of organisms on the composition of sea-water. In: Hill MN, editor. *The Sea*. Volume 2. New York: John Wiley. p 26-77.

Rey F. 1981a. Primary production estimates in the Norwegian Coastal Current between 62°N and 72°N. In: Sætre R, Mork M, editors. *The Norwegian Coastal Current*. University of Bergen. p 640-648.

Rey F. 1981b. The development of the spring phytoplankton outburst at selected sites off the Norwegian coast. In: Sætre R, Mork M, editors. *The Norwegian Coastal Current*. University of Bergen. p 649-680.

Sakshaug E, Slagstad D.1991. Light and productivity of phytoplankton in polar marine ecosystems: A physiological view. *Polar Research* 10:69-85.

Slagstad D, Downing K, Carlotti F, Hirche H-J. 1999. Modelling the carbon export and air-sea flux of CO_2 in the Greenland Sea. *Deep-Sea Research II* 46:1511-1530.

Slagstad D, Wassmann P. 1996. Climate change and carbon flux in the Barents Sea: 3-D simulations of ice-distribution, primary production and vertical export of particulate organic matter. *National Institute of Polar Research, Special Issue* 51:119-141.

Smith RC, Baker KS. 1981. Optical properties of the clearest natural waters (200-800 nm). *Applied Optics* 20:177-184.

Stoeker DK, Capuzzo JM. 1990. Predation on protozoa: its importance to zooplankton. *Journal of Plankton Research* 12:891-908.

Støle-Hansen K, Slagstad D. 1991. Simulation of currents, ice melting, and vertical mixing in the Barents Sea using a 3-D baroclinic model. *Polar Research* 10:33-44.

Sverdrup HU. 1953. On conditions for the vernal blooming of phytoplankton. *Journal du Conseil International pour l'Exploration de la Mer* 18:287-295.

Sætre R, Mork M. 1981. *The Norwegian Coastal Current*. University of Bergen. 795 p.

Tande KS. 1991. *Calanus* in high latitude environments. *Polar Research* 10:389-407.

Tollan A. 1974. River runoff in Norway. In: Skreslet S, editor. *Influence of freshwater outflow on biological processes in fjords and coastal waters*. New York: Springer-Verlag. p 11-13.

Urban-Rich J, Nordby E, Andreassen IJ, Wassmann P. 1999. Contribution by mesozooplankton fecal pellets to the carbon flux on Nordvestbanken, north Norwegian shelf in 1994. *Sarsia* 84:253-264.

Verity PG, Wassmann P, Ratkova TN, Andreassen IJ, Nordby E. 1999. Seasonal patterns in composition and biomass of autotrophic and heterotrophic nano- and microplankton communities on the north Norwegian shelf. *Sarsia* 84:265-277.

Walsh JJ.1988. *On the Nature of Continental Shelves*. London: Academic Press, Inc.

Walsh JJ, McRoy CP. 1986. Ecosystem analysis in the southeastern Bering Sea. *Continental Shelf Research* 5:259-288.

Wassmann P, Andreassen IJ, Rey F. 1999a. Seasonal variation of nutrients and suspended biomass on a transect across Nordvestbanken, north Norwegian shelf, in 1994. *Sarsia* 84:199-212.

Wassmann P, Hansen L, Andreassen IJ, Wexels Riser C, Urban-Rich J. 1999b. Distribution and sedimentation of faecal pellets on the Nordvestbanken shelf, northern Norway, in 1994. *Sarsia* 84:239-252.

Wassmann P, Slagstad D. 1993. Seasonal and annual dynamics of particulate carbon flux in the Barents Sea - A model approach. *Polar Biology* 13:363-372.

Wassmann P, Svendsen H, Keck A, Reigstad M. 1996. Selected aspects of the physical oceanography and particle fluxes in fjords of northern Norway. *Journal of Marine Systems* 8:53-71.

Whitledge TE, Reeburgh WS, Walsh, JJ. 1986. Seasonal inorganic nitrogen distribution and dynamics in the southeastern Bering Sea. *Continental Shelf Research* 5:109-132.

Accepted 18 June 1999 – Printed 15 November 1999
Editorial responsibility: Jarl Giske